TNFSF15 inhibits vasculogenesis by regulating relative levels of membrane-bound and soluble isoforms of VEGF receptor 1

Jian-Wei Qi, Ting-Ting Qin, Li-Xia Xu, Kun Zhang, Gui-Li Yang, Jie Li, Huai-Yuan Xiao, Zhi-Song Zhang[1], and Lu-Yuan Li[1]

State Key Laboratory of Medicinal Chemical Biology and Nankai University College of Pharmacy, and Tianjin Key Laboratory of Molecular Drug Research, Tianjin 300071, China

Edited by Napoleone Ferrara, University of California, San Diego, La Jolla, CA, and approved July 12, 2013 (received for review March 11, 2013)

Mouse bone marrow-derived Lin$^-$-Sca-1$^+$ endothelial progenitor cell (EPC) has pluripotent abilities such as supporting neovascularization. Vascular endothelial growth factor (VEGF) receptor 1 (VEGFR1) (Flt1) recognizes various VEGF isoforms and is critically implicated in a wide range of physiological and pathological settings, including vasculogenesis. Mouse EPC expresses two isoforms of VEGFR1: mFlt1, which transmits ligand-induced signals; and sFlt1, which acts as a negative regulator by sequestering ligands of VEGF receptors. How the relative levels of mFlt1 and sFlt1 are regulated is not yet clear. We report here that tumor necrosis factor superfamily 15 (TNFSF15) (also known as VEGI or TL1A), an endothelial cell-secreted cytokine, simultaneously promotes mFlt1 degradation and up-regulates sFlt1 expression in EPC, giving rise to disruption of VEGF- or PlGF-induced activation of eNOS and MAPK p38 and effective inhibition of VEGF-driven, EPC-supported vasculogenesis in a murine Matrigel implant model. TNFSF15 treatment of EPC cultures facilitates Akt deactivation-dependent, ubiquitin-assisted degradation of mFlt1 and stimulates sFlt1 expression by activating the PKC, Src, and Erk1/2 signaling pathway. Additionally, TNFSF15 promotes alternative splicing of the Flt1 gene in favor of sFlt1 production by down-regulating nuclear protein Jumonji domain-containing protein 6 (Jmjd6), thus alleviating Jmjd6-inhibited sFlt1 expression. These findings indicate that TNFSF15 is a key component of a molecular mechanism that negatively modulates EPC-supported vasculogenesis through regulation of the relative levels of mFlt1 and sFlt1 in EPC.

angiogenesis | protein degradation

Mouse bone marrow (BM)-derived lineage-negative, Sca-1–positive (Lin$^-$-Sca-1$^+$) progenitor cells have pluripotent abilities in hematopoiesis reconstitution (1), vasculogenesis (2), and tumor initiation (3). Functioning as endothelial progenitor cells (EPCs), these cells circulate to sites of vasculogenesis and differentiate in situ into endothelial cells (ECs) (2, 4). They also differentiate into ECs in culture (5, 6) and support tumor vasculogenesis in animal models (7–11). Functional incorporation of EPC into new blood vessels has been validated in clinical settings (12, 13) and murine models (7, 8, 14, 15).

Vascular endothelial growth factor (VEGF) and placenta growth factor (PlGF) promote vasculogenesis (14, 16–18). VEGF receptor 1 [VEGFR1 or fms-related tyrosine kinase 1 (Flt1)] is a receptor tyrosine kinase that mediates VEGF-A, VEGF-B, and PlGF-induced signals in a wide range of physiological and pathological settings of hematopoiesis and neovascularization (19–21). BM-derived VEGFR1$^+$ stem/progenitor cells promote tumor angiogenesis (22), initiate tumor premetastatic niche (23), and take part in reconstitution of hematopoiesis (1). The VEGFR1 gene has two products, membrane-bound mFlt1 and soluble sFlt1 (24). Membrane-bound mFlt1 is the full-length, fully functional VEGFR1. Soluble sFlt1 consists of only the extracellular domain of VEGFR1 and is incapable of transmitting signal across cell membrane. However, because of its high-affinity ligand binding ability, sFlt1 acts as a negative modulator by trapping VEGF-A, VEGF-B, and PlGF, preventing neovascularization promoted by these cytokines (25–27). It has been shown that sFlt1 inhibits tumor angiogenesis (28) and metastasis (29), binds lipid microdomains in kidney podocytes to control cell morphology and glomerular barrier function (30), regulates tip cell formation and branching morphogenesis in the zebra fish embryo (31), and plays a causal role in the pathogenesis of preeclampsia (32). In clinical settings, sFlt1 levels are of prognostic value in acute myocardial infarction (33).

The relative levels of mFlt1 and sFlt1 are closely regulated under specific physiological or pathological conditions. When ECs are exposed to VEGF, PI3K-Akt signals are activated to inhibit ubiquitin-assisted degradation of mFlt1 such that mFlt1 levels rapidly increase (34). Alternative splicing of the Flt1 gene is attributable to sFlt1 production (25, 35). The alternative splicing is regulated by Jumonji domain-containing protein 6 (Jmjd6) a nuclear protein that inhibits sFlt1 splicing (36). Despite the importance of the relative levels of proangiogenic mFlt1 and antiangiogenic sFlt1 in neovascularization, the molecular mechanism regulating concomitant changes of these two isoforms remains unclear.

Tumor necrosis factor superfamily 15 (TNFSF15) (also known as VEGI or TL1A), a cytokine produced predominantly by EC in established blood vessels, is a specific inhibitor of EC proliferation (37), being able to enforce growth arrest on quiescent EC but induce apoptosis in proliferating EC (38). Systemic administration of recombinant TNFSF15 led to inhibition of tumor angiogenesis and growth in animal models (39). It also inhibits Lin$^-$-Sca-1$^+$ EPC differentiation into EC (6) and EPC incorporation into tumor vasculature in murine models (10). TNFSF15 expression is absent or marginal in tumor vasculatures in various cancers (40–42), increased in irritable bowel syndrome (43), and down-regulated in wound tissues (44). TNFSF15 down-regulation in ovarian cancer is facilitated by VEGF secreted by cancer cells as well as by other inflammatory cytokines (42). Death domain-containing receptor 3 (DR3) (TNFRSF25), a member of the TNF receptor superfamily, has been shown to be the receptor of TNFSF15 in T cells and dendritic cells (45, 46).

We report here that TNFSF15 inhibits EPC-supported vasculogenesis by promoting ubiquitin-assisted degradation of mFlt1 while facilitating Flt1 gene transcription and alternative splicing toward increased sFlt1 production. These findings provide insights into a molecular mechanism that interlocks the actions of TNFSF15 and VEGFR1 signals.

Author contributions: J.-W.Q., Z.-S.Z., and L.-Y.L. designed research; J.-W.Q., T.-T.Q., L.-X.X., K.Z., G.-L.Y., and H.-Y.X. performed research; J.-W.Q. and L.-Y.L. contributed new reagents/analytic tools; J.-W.Q., J.L., Z.-S.Z., and L.-Y.L. analyzed data; and J.-W.Q. and L.-Y.L. wrote the paper.

The authors declare no conflict of interest.

This article is a PNAS Direct Submission.

[1]To whom correspondence may be addressed. E-mail: liluyuan@nankai.edu.cn or zzs@nankai.edu.cn.

This article contains supporting information online at www.pnas.org/lookup/suppl/doi:10.1073/pnas.1304529110/-/DCSupplemental.

CELL BIOLOGY

Results

TNFSF15 Inhibits EPC-Supported Vasculogenesis. To investigate TNFSF15 modulation of vasculogenesis in vivo, we injected a Matrigel solution containing VEGF (1 μg/mL), TNFSF15 (0.3 μg/mL), or vehicle, and freshly isolated green fluorescent protein (GFP)-marked, BM-derived Lin^--$Sca\text{-}1^+$ EPC s.c. into C57BL/6J mice. The animals were treated with TNFSF15 (5 mg/kg) or vehicle by i.p. injection 2 d before Matrigel implantation, and then daily for 6 d. When retrieved on day 7 postimplantation, the gel plugs from vehicle-treated animals became highly vascularized, whereas those from TNFSF15-treated animals remained clear with few blood vessels (Fig. 1*A*). Blood vessel densities on cross-sections of the vehicle-treated plugs were more than four times of that of TNFSF15-treated plugs (Fig. 1*B*). Superimposition of fluorescent confocal microscopic images of the cross-sections revealed that the new blood vessels (EC marker $CD31^+$) were formed by the implanted EPC (GFP^+), confirming that the implanted EPC differentiated into EC in the blood vessels ($CD31^+$-GPF^+, yellow) (Fig. 1*C*). A small number of the new blood vessels did not contain EPC-derived EC, and thus remained red-colored in the merged images. These data demonstrate that BM-derived EPCs are capable of supporting vasculogenesis and that TNFSF15 is able to inhibit EPC-supported vasculogenesis in this model.

TNFSF15 Inhibits Vasculogenesis Through Down-Regulation of mFlt1 and Up-Regulation of sFlt1. To determine the effect of TNFSF15 on mFlt1 and sFlt1 levels in VEGF-driven, EPC-supported vasculogenesis, we carried out immunofluorescent staining of the mFlt1 protein on frozen sections of the Matrigel plugs. We found that the mFlt1 protein diminished markedly as a result of TNFSF15 treatment (Fig. 2*A*). Fluorescence intensity assessment revealed that mFlt1 protein levels in vehicle-treated plugs were four times of that in TNFSF15-treated ones (Fig. 2*B*). We then digested the gel plugs, isolated the cells, labeled mFlt1 with allophycocyanin, and carried out flow-cytometric analysis (Fig. 2*C*). The percentage of mFlt1-positive cells in vehicle-treated plugs was three times that in TNFSF15-treated ones (Fig. 2*D*). We determined sFlt1 concentrations in cell-free supernatants of the digested plugs by ELISA and found that sFlt1 levels in TNFSF15-treated plugs were about three times that in vehicle-treated ones (Fig. 2*E*). Western blotting analysis of the plugs indicated that mFlt1 levels decreased by fivefold, whereas sFlt1 protein levels increased by sixfold (Fig. 2 *F* and *G*). These findings indicate that simultaneous down-regulation of mFlt1 and up-regulation of sFlt1 may attribute to TNFSF15 inhibition of vasculogenesis.

To determine whether down-regulation of mFlt1 or up-regulation of sFlt1 in EPC would lead to inhibition of vasculogenesis, we supplemented the EPC- and VEGF-containing Matrigel solution with mFlt1 siRNA (25 μg/mL) or recombinant sFlt1 (sFlt1-Fc, 25 μg/mL), or both. The gel plugs were retrieved on day 7. The mFlt1 siRNA treatment caused a substantial decline of mFlt1 (Fig. 2 *H* and *I*, and Fig. S1). Treatment with mFlt1 siRNA or sFlt1-Fc, either alone or together, led to significant inhibition of blood vessel formation (Fig. 2*J* and Fig. S1). These findings indicate that down-regulation of mFlt1 or up-regulation of sFlt1 can result in inhibition of VEGF-driven vasculogenesis.

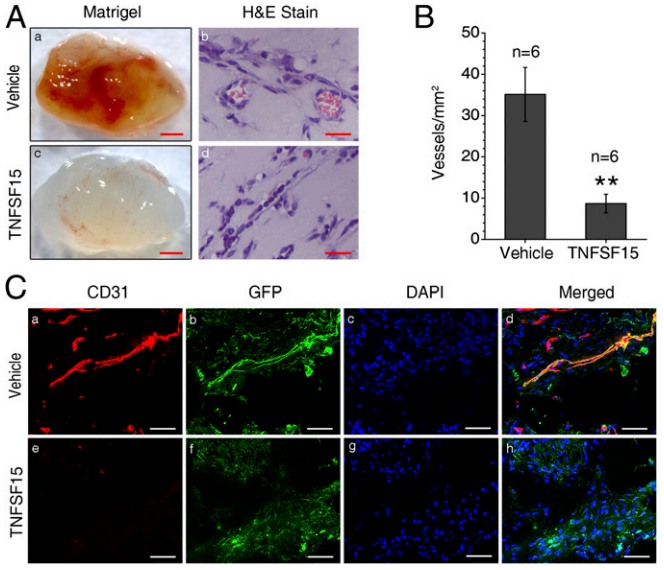

Fig. 1. TNFSF15 inhibition of VEGF-driven, EPC-supported vasculogenesis in Matrigel plugs. (*A*) Comparison of blood vessel formation in Matrigel plugs on experimental animals ($n = 6$ per group) treated with (*a* and *b*) vehicle or (*c* and *d*) TNFSF15 (5 mg/kg). (*a* and *c*) Typical images of Matrigel plugs from vehicle- or TNFSF15-treated groups. (Scale bar, 1 mm.) (*b* and *d*) H&E-stained cross-sections (5 μm) of the plugs from vehicle- or TNFSF15-treated groups. (Scale bar, 10 μm.) (*B*) Blood vessel densities of H&E-stained cross-sections of vehicle- or TNFSF15-treated plugs. (*C*) Fluorescent confocal microscopic images of frozen sections of Matrigel plugs from vehicle- or TNFSF15-treated groups. Red, CD31. Green, GFP. Blue, DAPI. Yellow, CD31-GFP double positive. (Scale bar, 50 μm.) The experiments were repeated once. Numbers on top of bars indicate the numbers of animals per group. Data are mean ± SD. $^{**}P < 0.01$, Student *t* test.

TNFSF15 Facilitates mFlt1 Down-Regulation and sFlt1 Up-Regulation in EPC. We treated freshly isolated mouse BM-derived Lin^--$Sca\text{-}1^+$ EPC with TNFSF15 (0.3 μg/mL, 30 min) and analyzed mFlt1 protein level in the cells by flow cytometry (Fig. 3*A*). The treatment led to a 66% down-modulation of mFlt1 (Fig. 3*B*). Presence of a TNFSF15 neutralizing antibody, 4-3H (0.4 mg/mL), in the culture media prevented the down-modulation (Fig. 3*B*). The blockage of TNFSF15-induced mFlt1 down-modulation by 4-3H was dose dependent (Fig. 3*C*). Using an antibody that recognizes both mFlt1 and sFlt1, we found by Western blotting analysis that the mFlt1 protein diminished within 30 min following TNFSF15 treatment and remained suppressed for at least 24 h, whereas cell-associated sFlt1 protein level increased significantly within 12 h and remained high at 24 h (Fig. 3*D*). We determined sFlt1 concentrations in EPC culture media by ELISA and found that within 24 h sFlt1 levels in TNFSF15-treated cultures increased by about twofold, whereas 4-3H effectively stopped the increase (Fig. 3*E*). By using RT-PCR, we found that TNFSF15 treatment gave rise to 7- and 15-fold increase of mFlt1 and sFlt1 mRNA levels, respectively, within 24 h (Fig. 3*F*). These findings indicate that TNFSF15 facilitates mFlt1 protein degradation, enhances sFlt1 secretion, and stimulates mFlt1 and sFlt1 mRNA production in EPC.

TNFSF15 Treatment Alters Signaling Pathways Regulating mFlt1 Degradation. The rapid mFlt1 degradation suggests an involvement of the ubiquitin–proteasome pathway. We thus treated EPC with ubiquitin inhibitor PYR-41 at various concentrations for 2 h before TNFSF15 treatment (0.3 μg/mL, 30 min). PYR-41 at 20 μM effectively prevented TNFSF15-stimulated mFlt1 degradation (Fig. 4*A*). We also treated EPC with proteasome inhibitor MG132 at various concentrations (2 h) before TNFSF15 treatment and found that MG132 also inhibited TNFSF15-induced mFlt1 degradation (Fig. 4*B*). To determine whether TNFSF15-induced mFlt1 degradation was reversible, we treated EPC with TNFSF15 for 30 min, and then replaced the culture media without TNFSF15. We found that mFlt1 protein level gradually restored upon TNFSF15 removal (Fig. 4*C*). Additionally, we found that TNFSF15-induced mFlt1 degradation was accompanied by Akt deactivation and that concomitant Akt reactivation and mFlt1 restoration occurred once TNFSF15 was removed (Fig. 4*C*). These data suggest that TNFSF15 treatment results in Akt deactivation, which is required for

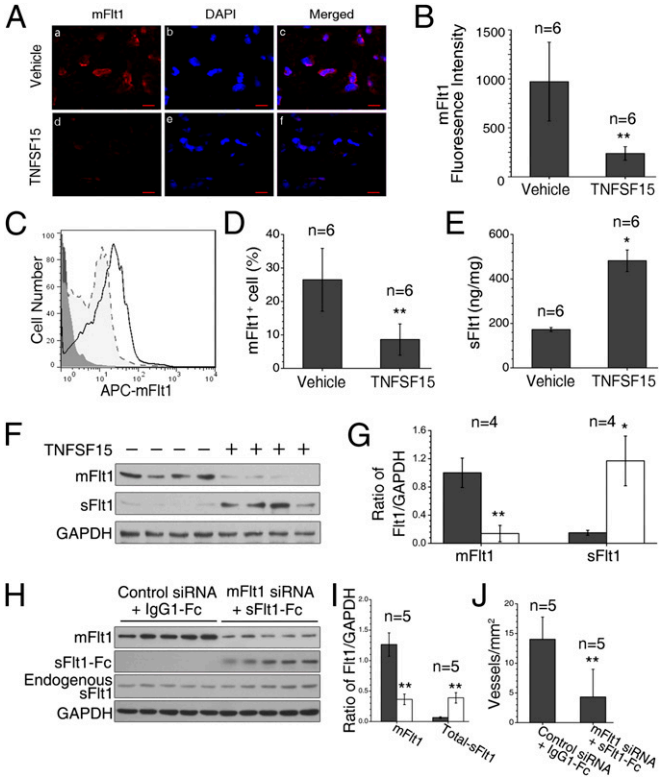

Fig. 2. TNFSF15-facilitated down-regulation of mFlt1 and up-regulation of sFlt1 in EPC in Matrigel plugs. (*A*) Fluorescent confocal microscopic images of mFlt1 staining of frozen Matrigel sections. Red, mFlt1$^+$ cells. Blue, nuclei. (Scale bar, 50 μm.) (*B*) Quantitative analysis of fluorescence intensities of mFlt1$^+$ cells. (*C*) FACS analysis of isolated EPC. Solid line, vehicle-treated. Dotted line, TNFSF15-treated. Gray line, isotype-matched antibody staining. (*D*) Percentages of mFlt1$^+$ cells determined by flow cytometry. (*E*) Concentrations of sFlt1 in supernatants of digested plugs, determined by ELISA. (*F*) mFlt1 and sFlt1 protein levels in individual plugs by Western blot. (*G*) Densitometry analysis of mFlt1 and sFlt1 protein bands in *F*. (*H*) mFlt1, sFlt1-Fc, and endogenous sFlt1 protein levels in individual gel plugs by Western blot. (*I*) Densitometry analysis of the protein bands in *H*; total sFlt1 indicates the sum of sFlt1-Fc and endogenous sFlt1. (*J*) Blood vessel densities in the gel plugs. The experiments were repeated two times. Numbers on top of bars indicate the numbers of animals per group. Data are mean ± SD. $*P < 0.05$, $**P < 0.01$, Student *t* test.

ubiquitin-assisted mFlt1 degradation. Because Akt is a substrate of phosphoinositol-3-kinase (PI3K), we pretreated EPC with PI3K inhibitor LY294002 (50 μM, 2 h) or DMSO, followed by treatment with TNFSF15. We found that LY294002 treatment effectively led to mFlt1 degradation and that TNFSF15 was no longer able to induce mFlt1 degradation in the presence of LY294002 (Fig. 4*D*). These findings are consistent with the view that TNFSF15-induced mFlt1 degradation in EPC is mediated through the ubiquitin–proteasome route, which is Akt deactivation dependent.

Intracellular Signaling Pathways Involved in TNFSF15-Stimulated sFlt1 Production in EPC. EC secretion of sFlt1 is promoted by the activation of PKC, Src, and Erk1/2 signals (47). To find out whether this signaling pathway is involved in TNFSF15-stimulated sFlt1 secretion by EPC, we treated the cells with PKC activator phorbol myristate acetate (PMA) (100 ng/mL, 2 h) or PKC inhibitor GF109203X (5 μM, 2 h), and then added TNFSF15 (0.3 μg/mL) to the media, and evaluated sFlt1 mRNA levels in 24 h by RT-PCR. PMA treatment led to an increase of sFlt1 mRNA with or without TNFSF15, whereas GF109203X suppressed TNFSF15-induced sFlt1 up-regulation (Fig. 5*A*). Antibody 4-3H inhibited TNFSF15-induced, but not PMA-induced, sFlt1 mRNA production. These findings suggest that TNFSF15 stimulation of sFlt1 production in EPC is mediated through the activation of PKC.

We then treated EPC with Src inhibitor PP2 (10 μM), Erk1/2 inhibitor U0126 (10 μM), or Akt inhibitor LY294002 (50 μM) for 2 h, and then with TNFSF15 or vehicle in the presence of each of the inhibitor for 24 h. RT-PCR analysis showed that PP2 and U0126 suppressed TNFSF15-induced sFlt1 up-regulation, whereas LY294002 had no effect (Fig. 5*B*). In addition, we treated the cells with 4-3H, GF109203X, or U0126 for 2 h, and then added TNFSF15, and analyzed in 6 h for phospho-Src by using flow cytometry (Fig. 5*C*). The percentage of phospho-Src–positive cells increased by 1.6-fold in response to TNFSF15, and the change was blocked by 4-3H or GF109203X, but not by U0126 (Fig. 5*D*). Moreover, we treated the cells with 4-3H, GF109203X, or PP2 for 2 h, and then added TNFSF15, and analyzed in 6 h for phospho-Erk1/2 by flow cytometry (Fig. 5*E*). The percentage of phospho-Erk1/2–positive cells increased by twofold upon TNFSF15 treatment; this enhancement diminished, however, when the cells were pretreated with 4-3H, GF109203X, or PP2 (Fig. 5*F*). These data indicate that TNFSF15-stimulated sFlt1 expression in EPC is mediated through the activation of PKC, Src, and Erk1/2. Because the

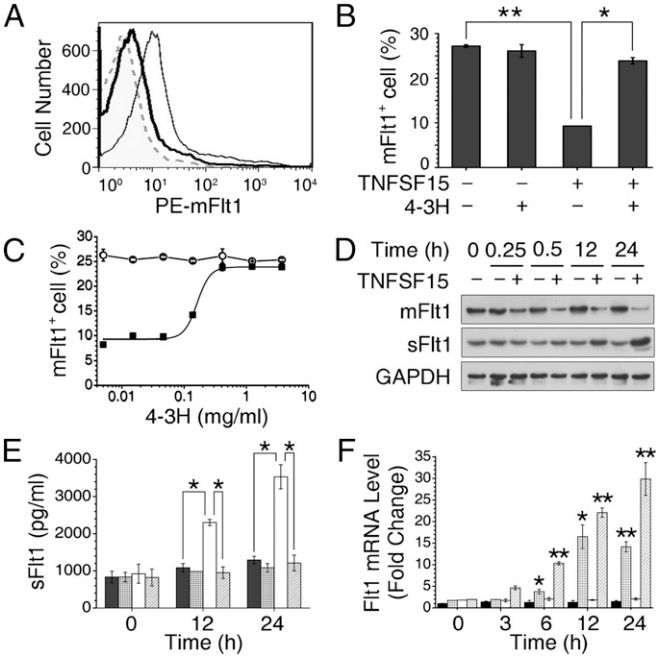

Fig. 3. TNFSF15-facilitated down-regulation of mFlt1 and up-regulation of sFlt1 in EPC cultures. (*A*) Flow cytometry histogram of Lin$^-$-Sca-1$^+$ EPC treated with TNFSF15 (bold line) or vehicle (thin line). The cells were labeled with a phycoerythrin-conjugated anti-mFlt1 antibody or an isotype-matched antibody (dotted line). (*B*) Percentages of mFlt1$^+$ cells in TNFSF15-treated cultures in the presence or absence of the TNFSF15 neutralizing antibody 4-3H, determined by flow cytometry. (*C*) Percentages of mFlt1$^+$ cells in TNFSF15 (squares)- or vehicle (circles)-treated cultures in the presence of 4-3H at indicated concentrations. (*D*) Western blotting analysis of mFlt1 and sFlt1 protein levels in TNFSF15- or vehicle-treated cultures at the indicated time points. (*E*) Concentrations of sFlt1 in culture media determined by ELISA at indicated time intervals following TNFSF15 treatment in the presence or absence of 4-3H; black, vehicle; crosses, 4-3H alone; white, TNFSF15 alone; slashes, TNFSF15 and 4-3H. (*F*) mRNA levels of mFlt1 and sFlt1 in TNFSF15- or vehicle-treated cultures at the indicated time points, determined by RT-PCR; black, mFlt1 in vehicle-treated cells; crosses, mFlt1 in TNFSF15-treated cells; white, sFlt1 in vehicle-treated cells; slashes, sFlt1 in TNFSF15-treated cells. The experiments were repeated two times. Data are mean ± SD. $*P < 0.05$, $**P < 0.01$, Student *t* test.

CELL BIOLOGY

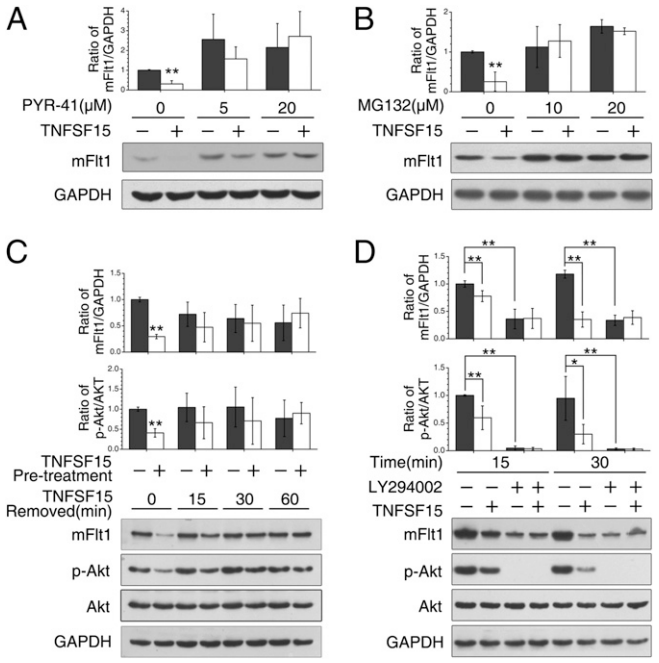

Fig. 4. Inhibition of PI3K/Akt activation in TNFSF15-stimulated, ubiquitin-assisted mFlt1 degradation in EPC. (*A*) Effect of ubiquitin inhibitor PYR-41 on TNFSF15-induced mFlt1 degradation. (*B*) Effect of proteasome inhibitor MG132 on TNFSF15-induced mFlt1 degradation. (*C*) Inhibition of Akt phosphorylation by TNFSF15 treatment and Akt rephosphorylation upon TNFSF15 removal. (*D*) Effect of PI3K inhibitor LY294002 on TNFSF15-induced mFlt1 degradation and Akt phosphorylation. Bar graphs represent quantitative analyses of Western blotting data from two independent experiments. Data are mean ± SD. $^{**}P < 0.01$, Student *t* test.

Erk inhibitor U0126 had no effect on TNFSF15-induced Src-phosphorylation, whereas the Src inhibitor PP2 effectively suppressed TNFSF15-induced Erk1/2-phosphorylation, the TNFSF15-activated signals proceeds along the PKC–Src–Erk1/2 axis.

Furthermore, we analyzed the effect of TNFSF15 action on Flt1 gene transcript alternative splicing. Because nuclear protein Jmjd6 inhibits sFlt1 mRNA production, we treated EPC with TNFSF15 for 6 h and analyzed Jmjd6 levels by immunofluorescent staining. TNFSF15 treatment resulted in marked decline of Jmjd6, which was restored by 4-3H (Fig. 5*G*). Quantitative analysis revealed an about 80% decrease of Jmjd6 fluorescence intensity (Fig. 5*H*). The inhibition of Jmjd6 activity by TNFSF15 was dose dependent, with an IC_{50} value of about 80 ng/mL (Fig. 5*I*). These findings indicate that TNFSF15 inhibits Jmjd6 activity, and this leads to a relief of Jmjd6-suppressed *Flt1* transcript splicing, giving rise to increased sFlt1 production.

TNFSF15 Suppresses EPC Response to VEGF or PlGF Stimulation. It is known that mFlt1 mediates VEGF-induced endothelial nitric oxide synthase (eNOS) and MAPK p38 phosphorylation in EC (19, 48), and that mFlt1 mediates PlGF-induced p38 activation (49). We treated the cells with TNFSF15 (0.3 μg/mL, 30 min), replaced the media without TNFSF15, and treated the cells with or without VEGF (10 ng/mL, 2 min) or PlGF (10 ng/mL, 5 min). We found that VEGF was no longer able to induce eNOS or p38 phosphorylation in TNFSF15-treated EPC until mFlt1 is restored upon TNFSF15 removal (Fig. 6*A*). Similarly, PlGF-induced activation of p38 was prevented by TNFSF15 treatment (Fig. 6*B*). As VEGFR2 may also transmit VEGF or PlGF activities, we determined VEGFR2 expression in freshly isolated EPC and found that the cells did not express VEGFR2 up to 6 d in culture (Fig. 6*C*). Thus, VEGFR2 is unlikely to account for the transmission of VEGF or PlGF signals in freshly isolated EPC. To determine the VEGF-sequestering ability of sFlt1 in TNFSF15-treated EPC, we analyzed VEGF interaction with sFlt1 in EPC culture media after 24 h treatment of the cells with TNFSF15. By carrying out Western blotting under nondenaturing conditions, we found a shift of VEGF from a free form (molecular mass, 50 kDa) to sFlt1-bound form (molecular mass, 110 kDa) (Fig. 6*D*). These findings indicate that TNFSF15-facilitated mFlt1 down-regulation and sFlt1 up-regulation leads to inhibition of EPC responsiveness to VEGF or PlGF.

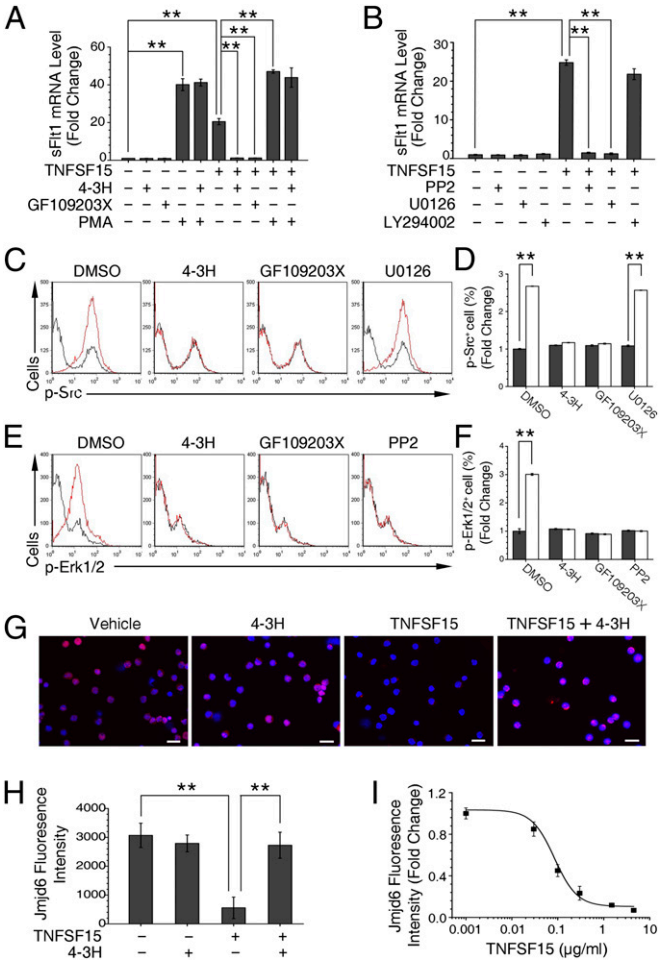

Fig. 5. TNFSF15-facilitated sFlt1 mRNA up-regulation and activation of PKC, Src, and Erk1/2 in EPC. (*A*) Changes of sFlt1 mRNA levels in response to TNFSF15 treatment in the presence or absence of 4-3H, GF109203X, or PMA, determined by real-time PCR. (*B*) Changes of sFlt1 mRNA levels in response to TNFSF15 treatment in the presence or absence of PP2, U0126, or LY294002, determined by RT-PCR. (*C*) Flow-cytometric analysis of Src phosphorylation in response to TNFSF15 treatment in the presence or absence of 4-3H, GF109203X, or U0126. Black lines, vehicle treated. Red lines, TNFSF15 treated. (*D*) Quantitative analysis of the data in *C*. Black bars, vehicle treated. White bars, TNFSF15 treated. (*E*) Flow-cytometric analysis of Erk1/2 phosphorylation in response to TNFSF15 treatment in the presence or absence of 4-3H, GF109203X, or PP2. Black lines, vehicle treated. Red lines, TNFSF15 treated. (*F*) Quantitative analysis of the data in *E*. Black bars, vehicle treated. White bars, TNFSF15 treated. (*G*) Microscopic images of Jmjd6 immunofluorescent staining of cells treated with TNFSF15 or vehicle for 6 h in the presence or absence of 4-3H; red, Jmjd6; blue, DAPI-stained nuclei. (Scale bar, 20 μm.) (*H*) Fluorescence intensity of Jmjd6 in TNFSF15-treated cells in the presence or absence of 4-3H. (*I*) Changes of Jmjd6 fluorescent intensity in EPC in response to TNFSF15 treatment. The experiments were repeated two times. Data are mean ± SD. $^{**}P < 0.01$, Student *t* test.

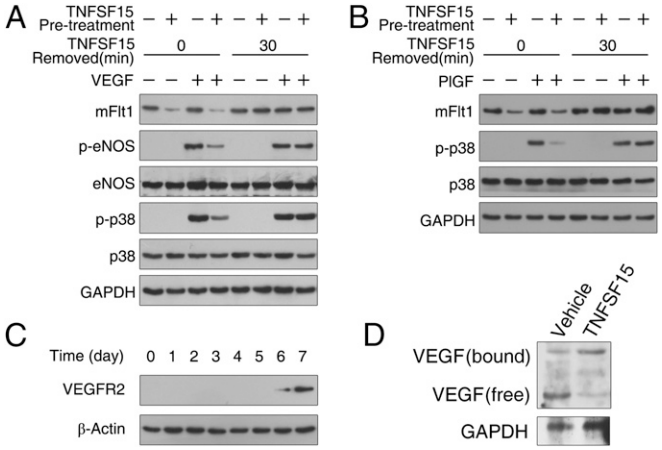

Fig. 6. TNFSF15 suppresses EPC response to VEGF and PlGF stimulation. Images of Western blotting analysis are shown. (*A*) Inhibition of VEGF-induced activation of eNOS and MAPK p38. (*B*) Inhibition of PlGF-induced activation of MAPK p38. (*C*) Time course of VEGFR2 expression in EPC. (*D*) VEGF interaction with sFlt1 in TNFSF15-treated (0.3 μg/mL, 24 h) EPC culture media; free and sFlt1-bound VEGF are identified. The experiments were repeated two times.

Discussion

Our data demonstrate that TNFSF15 simultaneously down-regulates mFlt1 and up-regulates sFlt1 levels in EPC. The regulation plausibly involves three pathways (Fig. 7). First, TNFSF15 promotes Akt deactivation-dependent, ubiquitin-mediated mFlt1 protein degradation. Second, TNFSF15 stimulates mFlt1 and sFlt1 mRNA transcription by activating the PKC–Src–Erk1/2 signaling axis. Third, TNFSF15 induces Jmjd6 down-regulation and thus alleviates Jmjd6 inhibition of *Flt1* transcript differential splicing toward sFlt1, enhancing sFlt1 production. These findings are highly significant in twofold. First, they show that the activity of the VEGF–VEGFR1 signaling pathway on EPC-supported vasculogenesis can be directly regulated by TNFSF15, a negative modulator of angiogenesis produced largely by EC in a normal vasculature. Second, the findings reveal a mechanism in which the production of the two VEGFR1 isoforms in EPC can be regulated simultaneously by TNFSF15, with an outcome in favor of an inhibition of EPC-supported vasculogenesis.

We showed previously that TNFSF15 gene expression in EC is down-regulated by VEGF produced by ovarian cancer cells (42). This indicates that the actions of a positive modulator of angiogenesis, namely VEGF, may lead to the removal from tumor microenvironment of a negative modulator of angiogenesis, namely TNFSF15, which would otherwise functions as an obstacle in the initiation or continuation of tumor angiogenesis. Our findings that TNFSF15 inhibits VEGF-induced vasculogenesis by simultaneously down-regulating mFlt1 and up-regulating sFlt1 point to the presence of a mechanism in which the actions of TNFSF15 and VEGF are interlocked. It is plausible that this mechanism is a critical component of the "angiogenesis switch" proposed by Folkman and Hanahan two decades ago (50). Further investigation of the interlocked actions of TNFSF15 and VEGF may help to materialize the angiogenesis switch at molecular level.

The paracrine and autocrine aspects of the actions of TNFSF15, VEGF, sFlt1, and mFlt1 on EPC are important because the initiation of new blood vessel formation is the result of joint actions of mFlt1- or sFlt1-expressing EPC, TNFSF15-producing EC, VEGF- or PlGF-producing cells such as inflammatory immune cells, other stromal cells, or cancer cells, at the site of vascular repair or in the tumor microenvironment. Under physiological conditions, TNFSF15 is mainly secreted by EC in established blood vessels. The action of EC-secreted TNFSF15 on EPC facilitates sFlt1 autocrine and down-regulates mFlt1 at the same time, diminishing EPC responsiveness to VEGF, a major stimulus of EPC proliferation and differentiation. Under pathological conditions such as in ischemic tissues or cancer lesions, however, TNFSF15 expression in EC is down-regulated by VEGF prominently secreted by hypoxic EC or cancer cells. Down-modulation of TNFSF15 will not only relieve an inhibition on EPC differentiation into EC, but also lead to reduced sFlt1 production by EPC, thus enhancing EPC responsiveness to VEGF, facilitating EPC participation in neovascularization. A cell surface receptor mediating TNFSF15 action on EPC is yet to be identified, because the currently known TNFSF15 receptor DR3 is not expressed in freshly isolated EPC, as we reported previously (6) and confirmed in this study (Fig. S2).

It is interesting to notice that TNFSF15 treatment leads to a rapid degradation of the mFlt1 protein and at the same time a significant increase of both mFlt1 and sFlt1 mRNA. The latter is likely due to a common transcription initiation site in the Flt1 gene for the transcription of both mFlt1 and sFlt1 (51), causing concomitant expression of sFlt1 and mFlt1. TNFSF15 inhibition on Jmjd6 activity encourages a shift of *Flt1* alternative splicing toward sFlt1 mRNA production.

In summary, this study reveals a mechanism underlying the modulation of vasculogenesis supported by EPC. Our finding that TNFSF15 treatment of EPC results in a shift of mFlt1 and sFlt1 balance in favor of sFlt1 secretion is significant because the relative levels of the two isoforms of VEGFR1 are a critical attribute in determining the activities of growth factors such as VEGF and PlGF in organ generation, tissue repair, as well as in tumor neovascularization.

Materials and Methods

Cells. Mouse BM-derived Lin^--Sca-1^+ EPCs were isolated as described (6). Briefly, BM cells were depleted of erythrocytes by hypotonic lyses. Lin^- cells were separated by negative selection using the Mouse Hematopoietic Progenitor Cell Enrichment Kit (StemCell). The cells were labeled with biotinylated Sca-1 antibody and isolated with streptavidin magnetic particles. EPCs were

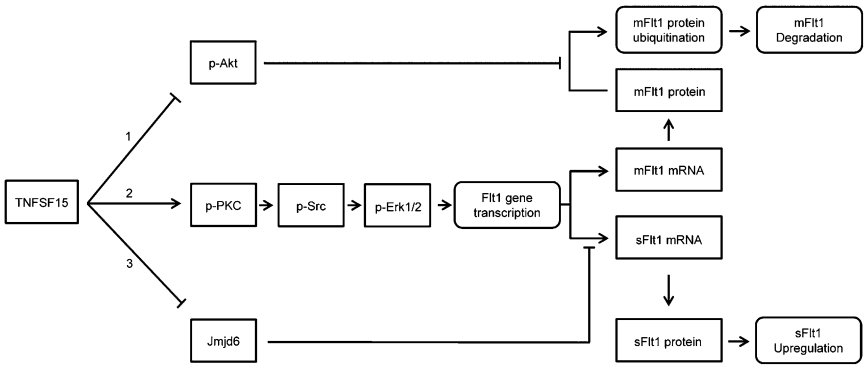

Fig. 7. A schematic presentation of plausible signaling pathways involved in TNFSF15 down-regulation of mFlt1 and up-regulation of sFlt1.

resuspended in endothelial growth medium (EGM-2) supplemented with EGF, hydrocortisone, VEGF, bFGF, heparin, IGF, gentamicin, and 5% FBS (Lonza), and cultured on fibronectin (10 μg/mL)-coated plates.

Matrigel Vasculogenesis Model. Freshly isolated EPCs were resuspended on ice in phenol red-free Matrigel solution and implanted into female C57BL/6J mice by abdominal s.c. injection (200 μL). Matrigel plugs were retrieved on day 7 after implantation, photographed with a Leica M165FC stereoscopic microscope, and each divided into four portions for hematoxylin and eosin staining, fluorescent immunostaining, recovering the cells and preparing cell-free homogenates, and Western blotting.

Statistical Analysis. The data were subjected to variance analysis (ANOVA), followed by two-tailed, unpaired Student *t* test. Differences with *P* values less than 0.05 were considered to be statistically significant.

Other reagents and experimental procedures are included in *SI Materials and Methods*.

ACKNOWLEDGMENTS. This study was supported in part by grants from The Ministry of Science and Technology of China (2009CB918901 and 2013ZX09103003-013 to L.-Y.L.), Natural Science Foundation of China (81272356 to L.-Y.L. and 81101709 to Z.-S.Z.), and Tianjin Municipality Science and Technology Commission (10ZCKFSH00100 to L.-Y.L.).

1. Hattori K, et al. (2002) Placental growth factor reconstitutes hematopoiesis by recruiting VEGFR1(+) stem cells from bone-marrow microenvironment. *Nat Med* 8(8):841–849.
2. Chavakis E, et al. (2005) Role of β2-integrins for homing and neovascularization capacity of endothelial progenitor cells. *J Exp Med* 201(1):63–72.
3. Mulholland DJ, et al. (2009) Lin-Sca-1+CD49fhigh stem/progenitors are tumor-initiating cells in the Pten-null prostate cancer model. *Cancer Res* 69(22):8555–8562.
4. van Solingen C, et al. (2011) MicroRNA-126 modulates endothelial SDF-1 expression and mobilization of Sca-1(+)/Lin(–) progenitor cells in ischaemia. *Cardiovasc Res* 92(3):449–455.
5. Bailey AS, et al. (2006) Myeloid lineage progenitors give rise to vascular endothelium. *Proc Natl Acad Sci USA* 103(35):13156–13161.
6. Tian F, Liang PH, Li L-Y (2009) Inhibition of endothelial progenitor cell differentiation by VEGI. *Blood* 113(21):5352–5360.
7. Bertolini F, Shaked Y, Mancuso P, Kerbel RS (2006) The multifaceted circulating endothelial cell in cancer: Towards marker and target identification. *Nat Rev Cancer* 6(11):835–845.
8. Gao D, et al. (2008) Endothelial progenitor cells control the angiogenic switch in mouse lung metastasis. *Science* 319(5860):195–198.
9. Spring H, Schüler T, Arnold B, Hämmerling GJ, Ganss R (2005) Chemokines direct endothelial progenitors into tumor neovessels. *Proc Natl Acad Sci USA* 102(50): 18111–18116.
10. Liang PH, et al. (2011) Vascular endothelial growth inhibitor (VEGI; TNFSF15) inhibits bone marrow-derived endothelial progenitor cell incorporation into Lewis lung carcinoma tumors. *Angiogenesis* 14(1):61–68.
11. Plummer PN, et al. (2013) MicroRNAs regulate tumor angiogenesis modulated by endothelial progenitor cells. *Cancer Res* 73(1):341–352.
12. Peters BA, et al. (2005) Contribution of bone marrow-derived endothelial cells to human tumor vasculature. *Nat Med* 11(3):261–262.
13. Fadini GP, Losordo D, Dimmeler S (2012) Critical reevaluation of endothelial progenitor cell phenotypes for therapeutic and diagnostic use. *Circ Res* 110(4):624–637.
14. Jujo K, et al. (2010) CXCR4 blockade augments bone marrow progenitor cell recruitment to the neovasculature and reduces mortality after myocardial infarction. *Proc Natl Acad Sci USA* 107(24):11008–11013.
15. Mellick AS, et al. (2010) Using the transcription factor inhibitor of DNA binding 1 to selectively target endothelial progenitor cells offers novel strategies to inhibit tumor angiogenesis and growth. *Cancer Res* 70(18):7273–7282.
16. Li B, et al. (2006) VEGF and PlGF promote adult vasculogenesis by enhancing EPC recruitment and vessel formation at the site of tumor neovascularization. *FASEB J* 20(9):1495–1497.
17. Rudge JS, et al. (2007) VEGF Trap complex formation measures production rates of VEGF, providing a biomarker for predicting efficacious angiogenic blockade. *Proc Natl Acad Sci USA* 104(47):18363–18370.
18. Ferrara N, Gerber HP, LeCouter J (2003) The biology of VEGF and its receptors. *Nat Med* 9(6):669–676.
19. Olsson AK, Dimberg A, Kreuger J, Claesson-Welsh L (2006) VEGF receptor signalling—in control of vascular function. *Nat Rev Mol Cell Biol* 7(5):359–371.
20. Pitchford SC, Lodie T, Rankin SM (2012) VEGFR1 stimulates a CXCR4-dependent translocation of megakaryocytes to the vascular niche, enhancing platelet production in mice. *Blood* 120(14):2787–2795.
21. Boscolo E, Mulliken JB, Bischoff J (2011) VEGFR-1 mediates endothelial differentiation and formation of blood vessels in a murine model of infantile hemangioma. *Am J Pathol* 179(5):2266–2277.
22. Lyden D, et al. (2001) Impaired recruitment of bone-marrow-derived endothelial and hematopoietic precursor cells blocks tumor angiogenesis and growth. *Nat Med* 7(11): 1194–1201.
23. Kaplan RN, et al. (2005) VEGFR1-positive haematopoietic bone marrow progenitors initiate the pre-metastatic niche. *Nature* 438(7069):820–827.
24. Kappas NC, et al. (2008) The VEGF receptor Flt-1 spatially modulates Flk-1 signaling and blood vessel branching. *J Cell Biol* 181(5):847–858.
25. Kendall RL, Thomas KA (1993) Inhibition of vascular endothelial cell growth factor activity by an endogenously encoded soluble receptor. *Proc Natl Acad Sci USA* 90(22): 10705–10709.
26. Ambati BK, et al. (2006) Corneal avascularity is due to soluble VEGF receptor-1. *Nature* 443(7114):993–997.
27. Kaza E, et al. (2011) Up-regulation of soluble vascular endothelial growth factor receptor-1 prevents angiogenesis in hypertrophied myocardium. *Cardiovasc Res* 89(2):410–418.
28. Verrax J, et al. (2011) Delivery of soluble VEGF receptor 1 (sFlt1) by gene electrotransfer as a new antiangiogenic cancer therapy. *Mol Pharm* 8(3):701–708.
29. Hu M, et al. (2008) Anti-angiogenesis therapy based on the bone marrow-derived stromal cells genetically engineered to express sFlt-1 in mouse tumor model. *BMC Cancer* 8:306.
30. Jin J, et al. (2012) Soluble FLT1 binds lipid microdomains in podocytes to control cell morphology and glomerular barrier function. *Cell* 151(2):384–399.
31. Krueger J, et al. (2011) Flt1 acts as a negative regulator of tip cell formation and branching morphogenesis in the zebrafish embryo. *Development* 138(10):2111–2120.
32. Maynard SE, et al. (2003) Excess placental soluble fms-like tyrosine kinase 1 (sFlt1) may contribute to endothelial dysfunction, hypertension, and proteinuria in preeclampsia. *J Clin Invest* 111(5):649–658.
33. Hochholzer W, et al. (2011) Impact of soluble fms-like tyrosine kinase-1 and placental growth factor serum levels for risk stratification and early diagnosis in patients with suspected acute myocardial infarction. *Eur Heart J* 32(3):326–335.
34. Zhang Z, Neiva KG, Lingen MW, Ellis LM, Nör JE (2010) VEGF-dependent tumor angiogenesis requires inverse and reciprocal regulation of VEGFR1 and VEGFR2. *Cell Death Differ* 17(3):499–512.
35. Huckle WR, Roche RI (2004) Post-transcriptional control of expression of sFlt-1, an endogenous inhibitor of vascular endothelial growth factor. *J Cell Biochem* 93(1):120–132.
36. Boeckel J-N, et al. (2011) Jumonji domain-containing protein 6 (Jmjd6) is required for angiogenic sprouting and regulates splicing of VEGF-receptor 1. *Proc Natl Acad Sci USA* 108(8):3276–3281.
37. Chew LJ, et al. (2002) A novel secreted splice variant of vascular endothelial cell growth inhibitor. *FASEB J* 16(7):742–744.
38. Yu J, et al. (2001) Modulation of endothelial cell growth arrest and apoptosis by vascular endothelial growth inhibitor. *Circ Res* 89(12):1161–1167.
39. Hou W, Medynski D, Wu S, Lin X, Li LY (2005) VEGI-192, a new isoform of TNFSF15, specifically eliminates tumor vascular endothelial cells and suppresses tumor growth. *Clin Cancer Res* 11(15):5595–5602.
40. Parr C, Gan CH, Watkins G, Jiang WG (2006) Reduced vascular endothelial growth inhibitor (VEGI) expression is associated with poor prognosis in breast cancer patients. *Angiogenesis* 9(2):73–81.
41. Zhou J, et al. (2011) LITAF and TNFSF15, two downstream targets of AMPK, exert inhibitory effects on tumor growth. *Oncogene* 30(16):1892–1900.
42. Deng W, et al. (2012) Down-modulation of TNFSF15 in ovarian cancer by VEGF and MCP-1 is a pre-requisite for tumor neovascularization. *Angiogenesis* 15(1):71–85.
43. Swan C, et al. (2013) Identifying and testing candidate genetic polymorphisms in the irritable bowel syndrome (IBS): Association with TNFSF15 and TNFα. *Gut* 62(7):985–994.
44. Conway KP, Price P, Harding KG, Jiang WG (2007) The role of vascular endothelial growth inhibitor in wound healing. *Int Wound J* 4(1):55–64.
45. Migone T-S, et al. (2002) TL1A is a TNF-like ligand for DR3 and TR6/DcR3 and functions as a T cell costimulator. *Immunity* 16(3):479–492.
46. Tian F, et al. (2007) The endothelial cell-produced antiangiogenic cytokine vascular endothelial growth inhibitor induces dendritic cell maturation. *J Immunol* 179(6):3742–3751.
47. Al-Ani B, et al. (2010) Activation of proteinase-activated receptor 2 stimulates soluble vascular endothelial growth factor receptor 1 release via epidermal growth factor receptor transactivation in endothelial cells. *Hypertension* 55(3):689–697.
48. Ahmad S, et al. (2006) Direct evidence for endothelial vascular endothelial growth factor receptor-1 function in nitric oxide-mediated angiogenesis. *Circ Res* 99(7):715–722.
49. Tchaikovski V, Fellbrich G, Waltenberger J (2008) The molecular basis of VEGFR-1 signal transduction pathways in primary human monocytes. *Arterioscler Thromb Vasc Biol* 28(2):322–328.
50. Folkman J, Hanahan D (1991) Switch to the angiogenic phenotype during tumorigenesis. *Princess Takamatsu Symp* 22:339–347.
51. Thomas CP, Raikwar NS, Kelley EA, Liu KZ (2010) Alternate processing of Flt1 transcripts is directed by conserved cis-elements within an intronic region of FLT1 that reciprocally regulates splicing and polyadenylation. *Nucleic Acids Res* 38(15):5130–5140.